PR-4 | 111

MILITARY TECHNICAL COLLEGE

CAIRO - EGYPT

SUPERCRITICAL DROPLET COMBUSTION: A NUMERICAL ANALYSIS

A.M.SARHAN *, M.A.EL-SENBAWI **

ABSTRACT

The design of a liquid propellant rocket engine thrust chamber requires the knowledge of the atomized droplet time of burning and its maximum flame sheet diameter so that the combustor length and diameter can be determined. In this work, the modified Spalding's analysis at supercritical pressure and temperature is presented. A computer program is coded to solve for the droplet time of burning and maximum flame sheet diameter. This code is used to solve five particular cases of those propellants which are used the most in rocket propulsion.

INTRODUCTION

In the liquid propellant rocket engines; the bipropellant components (fuel and oxidizer) are injected into the combustor through a group of delicate elements called the injectors. These injectors atomize the propellant components into small droplets. The size of the droplets depends on both Weber and Reynolds numbers. The droplets are spatially distributed forming a so called droplet distribution pattern. The diameter of these droplets is usually varying from 50 μm up to 200 μm, Barrère [1].

The injection velocity of these droplets is varying between 30 and 45 m/s. In the case of smaller droplet sizes and higher injection speeds (i.e. where Weber number reaches 20); droplet oscillations might be expected, Kuo [2]. This case should be avoided.

Spalding [3] introduced a theoretical model solving the case of a single fuel droplet combustion in a quiescent atmosphere. In this case, the rate of droplet burning is controlled by the rate of vaporization of the fuel.

---

* Assistant Professor, Department of Rockets, Military Technical College, Cairo, Egypt.

** Head of Department of Rockets, Military Technical College, Cairo, Egypt.

When the droplet is burned at a rocket engine the pressure and temperature are usually high so that the droplet is above its critical condition and the liquid fuel droplet becomes in the gaseous state. In this case the rate of burning is controlled by the rate of diffusion rather than by the rate of vaporization, Spalding [4].

In most cases - except for Hydrogen-Oxygen or Hydrogen-Fluorine propellants - both boiling point and heat of vaporization of the oxidants are much lower than that of the fuels. Therefore, the fuel droplet is considered to burn in an oxidant-surrounding atmosphere. Contrarily, for hydrogen-Oxygen and Hydrogen-Fluorine, the oxidant droplet is to be considered as being burned in a fuel-surrounding atmosphere.

Sanders [5] studied the case of unsteady state droplet combustion by solving numerically the complete set of partial differential conservation equations of mass, momentum, energy and chemical species. The experimental study of Bonin [6] and Avedisian [7] confirmed the validity of Spalding model. To eliminate the buoyance effect of the hot gases on the assumed spherical shape of the flame sheet; Dryer [8] studied the droplet combustion in the middeck area of the space shuttle where the Earth's gravity can be ignored.

THEORETICAL MODEL

Spalding [3] solved the combustion of a fuel droplet surrounded by an oxidant environment. According to Spalding's model; the rate of the droplet combustion is controlled by the rate of vaporization of the fuel droplet. This case is usually referred to as the quasi steady theory of droplet combustion. In rocket or jet combustors; usually the pressure is above 2 MPa and the temperature is above 2000°K. This means that the pressure and temperature are always above the critical limits of the commonly used fuels, Fig.1. This implies that the latent heat of vaporization decreases to zero and the liquid droplet is transformed into the gaseous phase during a very short time. Therefore the droplet combustion is controlled by the rate of diffusion rather than by the rate of vaporization. Consequently, the supercritical bipropellant combustion reduces to the case of a pocket of fuel vapors surrounded by a spherical flame zone. These fuel vapors diffuse outward to the flame front. Outside the flame zone the oxidant diffuses inward to the flame front, where they react instantly to form combustion products.

Rosner [9] and Dominicis [10] modified the Spalding's analysis coming out with a modified model for supercritical bipropellant combustion.

The basic assumptions of this model are:

- The fluid properties are constant.
- The mass diffusivities of all species are identical, and only concentration diffusion is present in the system.
- The radial bulk velocity is zero.
- The reaction takes place in a thin flame zone.
- The combustion is a single one-step reaction ($\nu_f M_f + \nu_o M_o \longrightarrow \nu_p M_p$) where ν_f, ν_o, ν_p, M_f, M_o and M_p are the reaction coefficient and chemical formulae of fuel, oxidizer and product respectively.

The conservation of species i is given by:

$$\rho \frac{\partial Y_i}{\partial t} = \omega_i - \left[\nabla . (\rho Y_i \bar{V}_i)\right] \qquad (1)$$

Where

ρ Specific mass,
t time,
Y_i The mass fraction of the species i ($Y_i = \rho_i/\rho$) ,
ω_i The rate of generation of the species i,
$\bar{V}_i$ Diffusion velocity of species i.

The phenomenological chemical-kinetic expression is

$$\omega_i = W_i (\nu_i'' - \nu_i')\omega \qquad (2)$$

Where

ν_i'', ν_i' Stoichiometric coefficient of species i appearing as a product and reactant respectively,
W_i Molecular weight of species i,
ω Rate of reaction of the fuel with the oxidizer.

The constitutive diffusion relation is

$$\nabla X_i = \sum_{j=1}^{N} \frac{X_i X_j}{\mathcal{D}_{ij}} (\bar{V}_j - \bar{V}_i) \qquad (3)$$

Where

X_i, X_j The mole fractions i, j respectively,
$\mathcal{D}_{ij}$ Binary diffusion coefficient of the gases i, j.
$\bar{V}_i$, $\bar{V}_j$ Mass diffusion velocity of species i, j.
N Total number of species.

Using the second assumption, $\bar{V}_i$ and $\bar{V}_j$ can be expressed as:

$$\bar{V}_i = - \mathcal{D} \frac{\nabla Y_i}{Y_i} \tag{4}$$

substituting Eqs.2 and 4 into Eq.1 gives

$$W_i (\nu_i'' - \nu_i') = \rho \frac{\partial Y_i}{\partial t} - \nabla . (\rho \mathcal{D} \nabla Y_i) \tag{5}$$

Defining a new dependent variable

$$\alpha_i \equiv \frac{Y_i}{W_i (\nu_i'' - \nu_i')} \tag{6}$$

and substituting α_i for Y_i, Eq.5 becomes

$$\omega = \rho \frac{\partial \alpha_i}{\partial t} - \nabla . (\rho \mathcal{D} \nabla \alpha_i) \tag{7}$$

for i = f, O, or p.

Let $$\beta' \equiv \alpha_p - \alpha_f \tag{8}$$

$$\beta' = \frac{Y_p}{\nu_p W_p} + \frac{Y_f}{\nu_f W_f} \tag{8'}$$

Replacing α_p with β', Eq.7 becomes

$$\rho \frac{\partial \beta_i}{\partial t} = \nabla . (\rho \mathcal{D} \nabla \beta') \tag{9}$$

Let us define β_o' as the value of β' for $r \leq r_*$ at t = 0; then

$$\beta_o' \equiv \frac{1}{\nu_f W_f} \tag{10}$$

Also define β_∞' as r approaches ∞; then

$$\beta'_\infty \equiv \frac{Y_{p\infty}}{\nu_p W} \tag{11}$$

β'_∞ may be nonzero, because the gaseous mixture far from the droplet may have some constant concentration of products $Y_{p\infty}$.

If we further define a dependent variable

$$\Gamma \equiv \frac{\beta' - \beta'_\infty}{\beta'_o - \beta'_\infty} \tag{12}$$

and substitute Γ for β', Eq.9 becomes

$$\rho \frac{\partial \Gamma}{\partial t} = \nabla \cdot (\rho \mathcal{D} \nabla \beta') \tag{13}$$

In spherical coordinates, Eq.13 can be written as

$$\rho \frac{\partial \Gamma}{\partial t} = \frac{\mathcal{D} \rho}{r^2} \frac{\partial}{\partial r} \left(r^2 \frac{\partial \Gamma}{\partial r} \right) \tag{14}$$

The boundary condition at the far field is at $r \longrightarrow \infty$; $\Gamma = 0$.

The total mass of the single fuel droplet, M_t can be expressed as

$$M_t = \int_o^\infty 4 \pi r^2 \rho \left(Y_f + \frac{\nu_f W_f}{\nu_p W_p} Y_p \right) dr \tag{15}$$

The mass of the single fuel droplet, M_f, injected into the combustor at time $t = 0$ is

$$M_f = \int_o^\infty 4 \pi r^2 \rho \Gamma \, dr \tag{16}$$

The initial conditions at $t = 0$ are

at $r \leq r_{so}$: $\Gamma = 1$, at $r > r_{so}$: $\Gamma = 0$,

where r_{so} is the fuel droplet radius at $t = 0$.

The particular solution for Eq.14 is

$$\Gamma = \frac{M_f}{\rho (4 \pi \mathcal{D} t)^{3/2}} \exp \left(\frac{- r^2}{4 \mathcal{D} t} \right) \tag{17}$$

It should be noted that for times of order greater than $r_{so}^2/\mathcal{D}$ the fuel distribution is independent of whether the initial mass is concentrated at a point or is finitely distributed. It should also be noted that Eq.17 is unrealistic at $t \longrightarrow 0$.

To determine the location of the spherical flame front, r_{fl}, we can set $Y_f = 0$, $Y_o = 0$, and $Y_p = 1$. Also note that at infinity we have

$$Y_p + Y_o = 1 \tag{18}$$

The value of Γ at the flame front, Γ_{fl} can be calculated from Eq.12. It can also be expressed as

$$\Gamma_{fl} = \frac{Y_{o\infty}}{\left(\nu_o W_o / \nu_f W_f \right) + Y_{o\infty}} \tag{19}$$

Solving Eq.17 for r and setting $\Gamma = \Gamma_{fl}$, the flame front position is given as a function of time

$$r_{fl}^2 = 4 \mathcal{D} t \ln \left[\frac{M_f}{\rho \Gamma_{fl} (4 \pi \mathcal{D} t)^{3/2}} \right] \tag{20}$$

Defining the following two dimensionless variables as:

$$\phi \equiv \frac{r_{fl}}{\left(M_f / \rho \Gamma_{fl} \right)^{1/3}} \tag{21}$$

$$\theta \equiv \frac{4 \pi \mathcal{D} t}{\left(M_f / \rho \Gamma_{fl} \right)^{2/3}} \tag{22}$$

The dimensionless flame radius ϕ is shown in Fig.2 as a function of θ based upon the following equation deduced from Eq.20:

$$\phi = \left[- \left(\frac{3}{2\pi} \right) \theta \ln \theta \right]^{1/2} \tag{23}$$

The maximum flame radius can be shown to occur at $\theta = 0.368$ with $\phi_{max} = 0.419$. The maximum flame radius can also be expressed in terms of M_f, ρ and Γ_{fl} according to the following equation.

$$(r_{fl})_{max} = 0.419 \left(\frac{M_f}{\rho \Gamma_{fl}}\right)^{1/3} \tag{24}$$

and the time variation of the size of diffusion flame is shown in Fig.3. The total burning time, t_b, can be obtained by setting $r_{fl} = 0$ or $\phi = 0$. Corresponding to $\phi = 0$, θ must equal to 1 in Eq.23. Substituting $\theta = 1$ into Eq.22 ; one can obtain

$$t_b = \frac{\rho^{1/3} \left(M_f/\Gamma_{fl}\right)^{2/3}}{4 \pi (\rho \mathcal{D})} \tag{25}$$

The binary diffusion coefficient, $\mathcal{D}_{AB}$, of two gases A and B is given by

$$\mathcal{D}_{AB} = \frac{2}{3} \left(\frac{K}{\pi}\right)^{3/2} \frac{\left[\frac{1}{2} T^3 \left(\frac{1}{\mathcal{M}_A} + \frac{1}{\mathcal{M}_B}\right)\right]^{1/2}}{p \left(\frac{\sigma_A + \sigma_B}{2}\right)^2} \tag{26}$$

where K, σ_A , σ_B, $\mathcal{M}_A$ and $\mathcal{M}_B$ are the Boltzmann's constant and the molecular diameters and masses of the gases A and B respectively.

Faëth et al [11] conducted supercritical combustion tests at pressure of the order of 10 MPa under zero gravity. Their results generally confirm the present model.

To study the pressure dependence of t_b, one can rearrange Eq.25 to give

$$t_b \quad \alpha \quad p^{1/3} \tag{27}$$

The result that the burning time is proportional to $p^{1/3}$ obtained from the modified analyses of Rosner [9] and Dominicis [10] is essentially unchanged from that of Spalding's early theory of high-pressure droplet combustion [4]. This shows that, despite that the increase of the combustion chamber pressure enhances the specific impulse, it requires a longer combustor. It should be also noted that the greater the flame front radius of the fuel droplet, the greater the combustor diameter.

COMPUTATION ANALYSIS

A computer program following the introduced model is coded to solve for the time of burning and the maximum flame sheet diameter of any available bipropellant having known droplet size and known physical parameters. This code devices a subroutine

WEIN, Strehlow [12], to compute the adiabatic flame temperature and the composition and number of moles of the combustion gas products.

Sequence of the Computation

1. Thermochemical calculation of reaction of an almost stoichiometric mixture of the propellants being investigated. The input to this code is the summary formula of the propellant, its overall heat of formation and the combustion working pressure. The output of the computation is the adiabatic flame temperature, T_s, the gas products and the average molecular mass.

2. Computation of the adiabatic flame temperature, T_r, from the thermochemical calculation of reaction of the real mixing ratio of the propellant being investigated.

3. Computation of the average binary diffusion coefficient of the fuel with the gas products computed for the stoichiometric mixture. The binary diffusion coefficient is computed at the combustion chamber pressure and the temperature of the real mixing ratio, using Eq.26.

4. Computation of the dimensionless parameter Γ_{fl} using Eq.19.

5. For each droplet size; the maximum flame front radius, $(r_{fl})_{max}$, and time of burning t_b are computed using Eq.24 and Eq.25 respectively.

Computed Cases

According to the specific impulse; the propellants are usually categorized into:

1. Low energy propellants with specific impulse up to 2500 m/s.

2. Medium energy propellants with specific impulse ranging from 2500 m/s up to 3000 m/s.

3. High energy propellants with specific impulse higher than 3000 m/s.

The following five propellants are investigated:

Kerosene ($C_{10}H_{20}$) + Nitric acid (HNO_3)

Hydrazine (N_2H_4) + Nitric acid (HNO_3)

Hydrazine Hydrate (N_2H_4,H_2O) + Nitric acid (HNO_3)

Dimethyl-hydrazine ($C_2H_8N_2$) + Nitric acid (HNO_3)

Hydrogen (H_2) + Oxygen (O_2)

Computation analysis, at combustion pressure of 70 bar and pressure ratio of 1/70, of the stoichiometric mixtures of these propellants respectively gave the following:

Flame sheet temperatures: 2830, 2760, 2960, 3000 and 2710 °K.
Specific impulse: 2430, 2600, 2740, 2540 and 3350 m/s.

The first propellant represents the low energy category. It is usually used in the short range missiles. The second, third and forth propellants represent the medium energy category. These are usually used for the medium range missiles. The fifth propellant represents the high energy category. It is usually used for the long range missiles or for the space launching vehicles.

Results of the computational analysis of droplet combustion with initial radii ranging from 10 - 100 μm of these five propellants are presented in Fig.4 and Fig.5.

Fig.4. shows the burning time versus the initial droplet radius. This shows that Kerosene propellant requires the longest combustors, while Hydrogen propellant requires the shortest combustors, and the Hydrazines require a medium length combustor.

Fig.5. shows the maximum flame sheet radius versus the initial droplet radius. This shows that Kerosene propellant requires the greatest combustor diameter, while Hydrogen propellants the smallest one. The Hydrazines propellants require a medium combustor diameter.

The comparison of the computed data with the dimensions of thrust chambers of available existing rockets confirmed the accuracy and usefulness of the computer code based on the presented analysis.

CONCLUSION

The presented code is a useful tool for the computation of droplet burning time which is important to determine the combustor length which ensures complete combustion.

It also computes the maximum flame sheet diameter which is important to determine the combustor diameter required to secure combustion without flame sheet interference. Consequently, stable combustion can be maintained.

REFERENCES

1. Barrère.M. 'Rocket Propulsion', Elsevier, 1960.

2. Kuo, K.K. 'Principles of Combustion', 2nd ed. p.520, John Wiley & Sons, New York, 1986.

3. Spalding, D.B. 'Droplet Combustion', Fourth International Symposium in Combustion, p.847, 1953.

4. Spalding, D.B. 'Theory of Particle Combustion at High Pressures', ARS J., pp.828-835, November 1959.

5. Sanders, B.R. and Dwyer,H.A. 'Modeling Unsteady Droplet Combustion Processes' ASME pp.3-10, New York, 1988.

6. Bonin,M.P. and Queiroz,M. 'Analysis of Single Stream Droplet Combustion through Size and Velocity Measurements', ASME pp.3-8, New York, 1991.

7. Avedisian,C.T.,Yang,J.C. and Wang,C.H.,' On Low Gravity Droplet Combustion' Proc. R. Soc., London. Ser.A., Vol.420, n.1858, pp.183-200, Nov.1988

8. Dryer, F.L. and Williams, F.A.,'Droplet Combustion at Reduced Gravity' NASA Tech. Memo. V.2, n.4069, pp.675-691, Oct.,1988.

9. Rosner,D.E.,'On Liquid Droplet Combustion at High Pressure', AIAA J.,Vol.5,No.1.,pp.165-168, 1967.

10. Dominicis, D.P.,'An Experimental Investigation of Near Critical and Supercritical Burning of Bipropellant Droplets', NASA CR-72399, 1968.

11. Faeth, G.M., Dominicis, D.P., Tulpinsky,J.F. and Olson,D.R., 'Supercritical Bipropellant Droplet Combustion', Twelveth International Symposium in Combustion, pp.9-18,1969.

12. Strehlow, R.A.,'Combustion Fundamentals', McGraw-Hill, 1984.

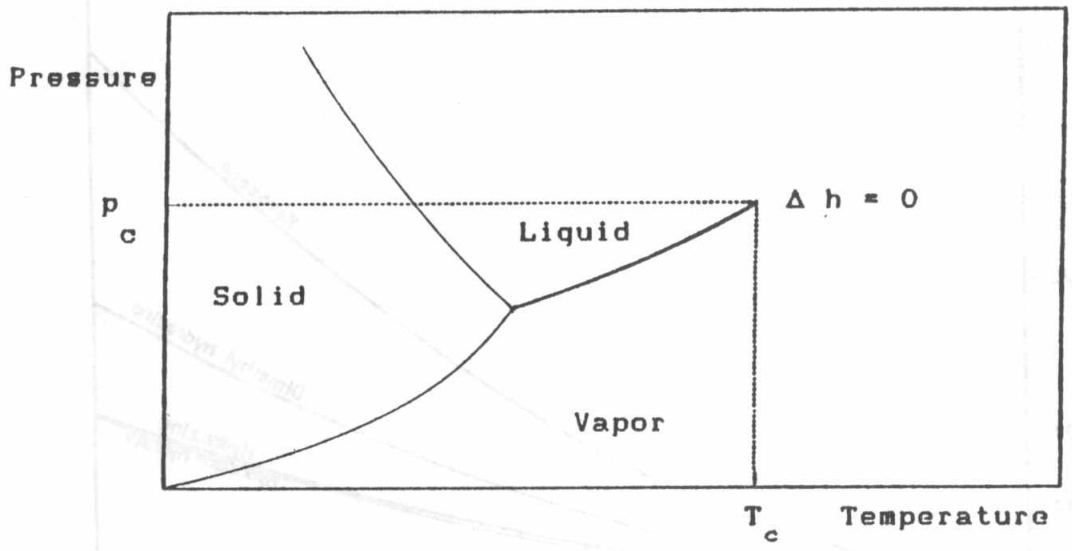

Figure 1. Phase diagram of a liquid fuel

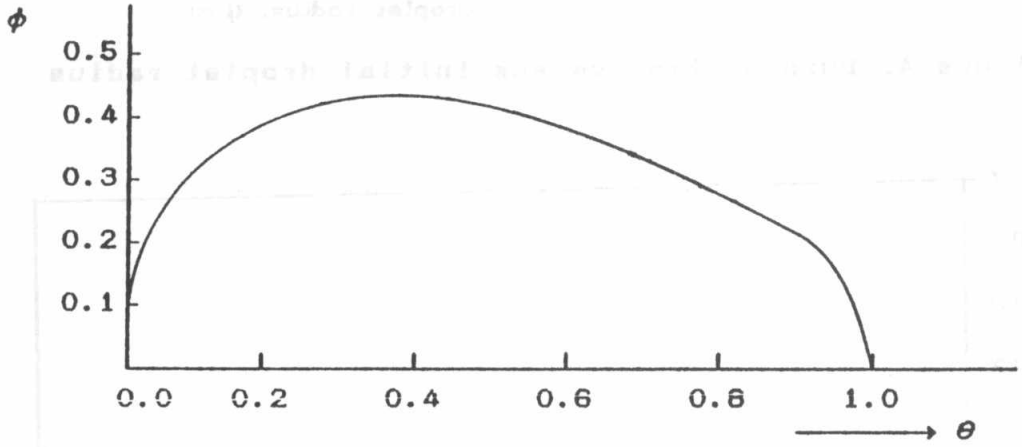

Figure 2 Radius of flame front versus time (after Spalding [4]).

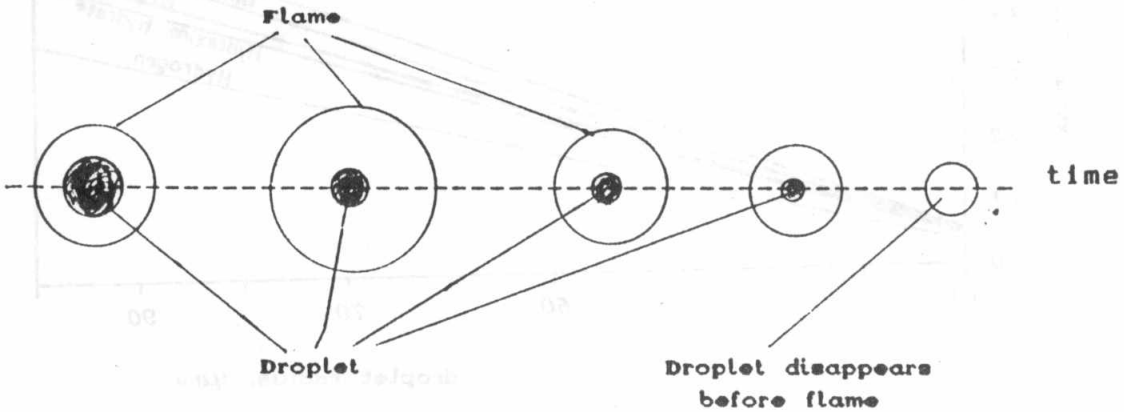

Figure 3. Appearance of burning droplets under transient condition (after Spalding [4]).

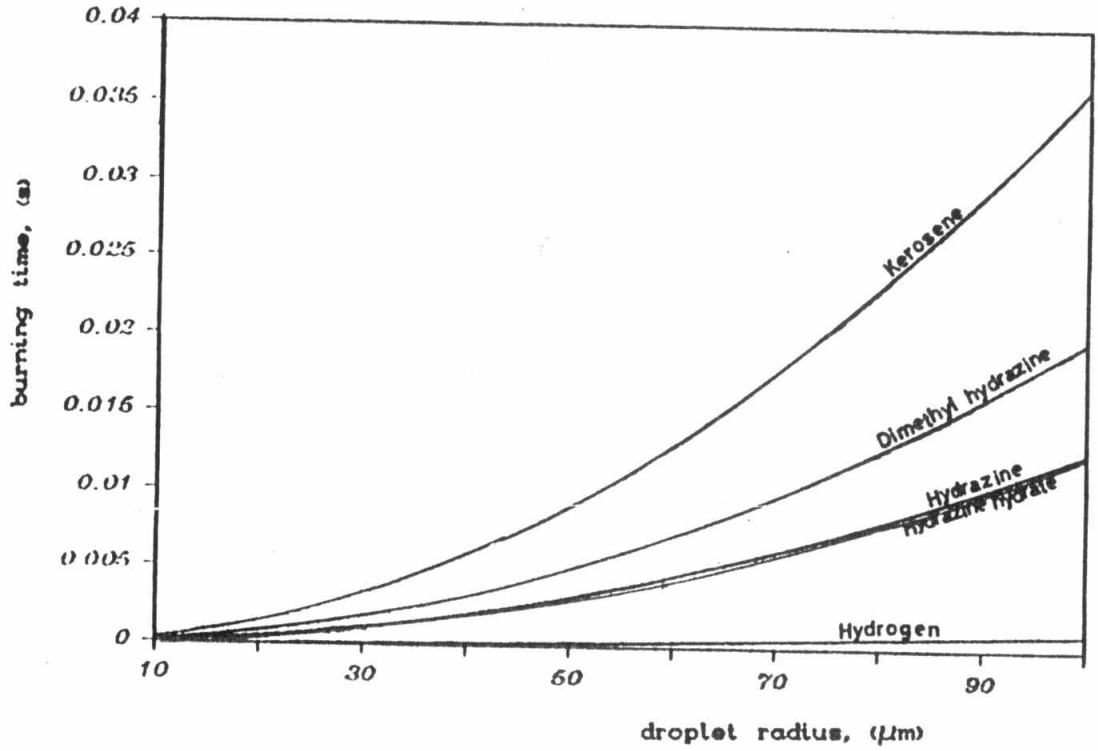

Figure 4. Burning time versus initial droplet radius

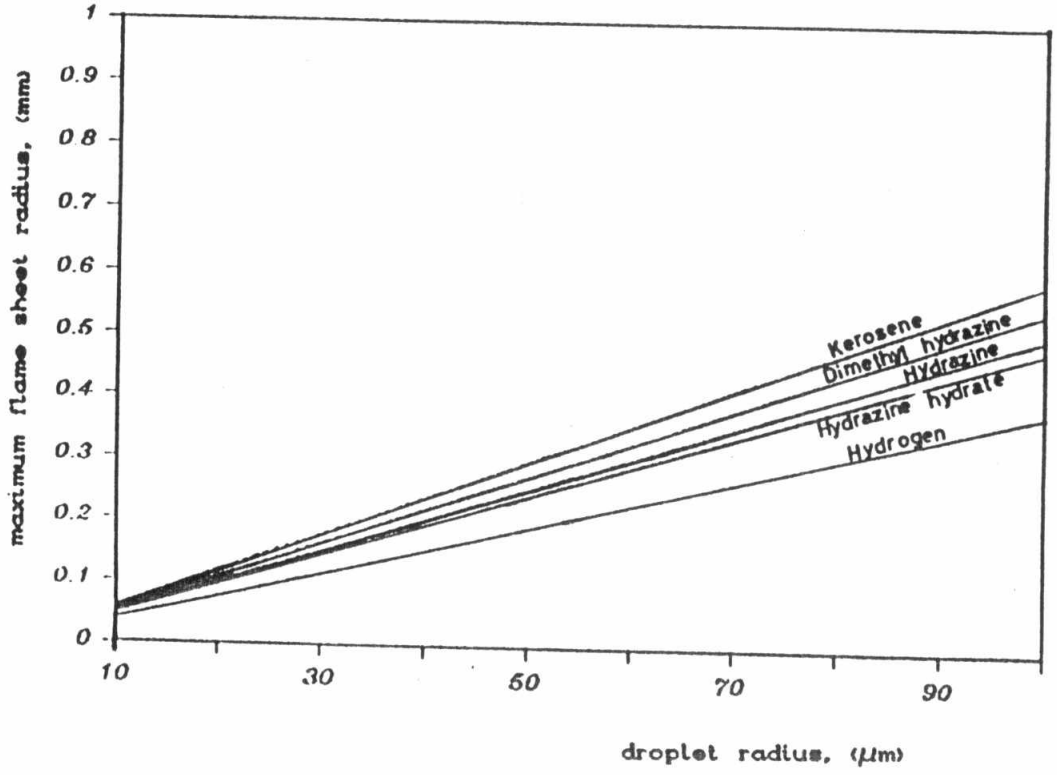

Figure 5. Maximum flame sheet radius versus initial droplet radius